

Tight-binding modelling of the electronic band structure of layered superconducting perovskites

T Mishonov[†] and E Penev

Laboratorium voor Vaste-Stoffysica en Magnetisme, Katholieke Universiteit Leuven, Celestijnenlaan 200 D, B-3001 Leuven, Belgium

Received 9 March 1999, in final form 22 September 1999

Abstract. A detailed tight-binding analysis of the electron band structure of the CuO_2 plane of layered cuprates is performed within a σ -band Hamiltonian including four orbitals – $\text{Cu}3d_{x^2-y^2}$, $\text{Cu}4s$, $\text{O}2p_x$, and $\text{O}2p_y$. Both the experimental and theoretical hints in favor of Fermi level located in a Cu or O band, respectively, are considered. For these two alternatives analytical expressions are obtained for the LCAO electron wave functions suitable for the treatment of electron superexchange. Simple formulae for the Fermi surface and electron dispersions are derived by applying the Löwdin down-fold procedure to set up the effective copper and oxygen Hamiltonians. They are used to fit the experimental ARUPS Fermi surface of $\text{Pb}_{0.42}\text{Bi}_{1.73}\text{Sr}_{1.94}\text{Ca}_{1.3}\text{Cu}_{1.92}\text{O}_{8+x}$ and both the ARPES and LDA Fermi surface of $\text{Nd}_{2-x}\text{Ce}_x\text{CuO}_{4-\delta}$. The value of presenting the hopping amplitudes as surface integrals of *ab initio* atomic wave functions is demonstrated as well. The same approach is applied to the RuO_2 plane of the ruthenate Sr_2RuO_4 . The LCAO Hamiltonians including the three in-plane π -orbitals $\text{Ru}4d_{xy}$, O_a2p_y , O_b2p_x and the four transversal π -orbitals $\text{Ru}4d_{zx}$, $\text{Ru}4d_{yz}$, O_a2p_z , O_b2p_z , are separately considered. It is shown that the equation for the constant energy curves and the Fermi contours has the same canonical form as the one for the layered cuprates.

PACS numbers: 74.25.Jb, 71.25.Pi, 74.72.-h

Submitted to: *J. Phys.: Condens. Matter*

Published in *J. Phys.: Condens. Matter* **12** (2000), pp. 143–159

[†] Permanent address: Department of Theoretical Physics, Faculty of Physics, University of Sofia, 5 J. Bourchier Blvd., 1164 Sofia, Bulgaria

1. Introduction

After the discovery of the high- T_c superconductors the layered cuprates became one of the most studied materials in the solid state physics. A vast range of compounds were synthesised and their properties comprehensively investigated. The electron band structure is of particular importance for understanding the nature of superconductivity in this type of perovskites [1]. Along this line one can single out the significant success achieved in the attempts to reconcile the photoelectron spectroscopy data [2] and the band structure calculations of the Fermi surface (FS) especially for compounds with simple structure such as $\text{Nd}_{2-x}\text{Ce}_x\text{CuO}_{4-\delta}$ [3, 4]. A qualitative understanding, at least for the self-consistent electron picture, has been achieved and for the most electron processes in the layered perovskites one can employ adequate lattice models.

There is not much analysis of the electronic band structures of the high- T_c materials in the terms of single analytical expressions available. This is something for which there is a clear need, in particular to help in the construction of more realistic many-body Hamiltonians. The aim of this paper is to analyse the common features in the electron band structure of the layered perovskites within the tight-binding (TB) method [5]. In the following we shall focus on the metallic (being eventually superconducting) phase only, with the reservation that the antiferromagnetic correlations, especially in the dielectric phase, could substantially change the electron dispersions. It is shown that the linear combination of atomic orbitals (LCAO) approximation can be considered as an adequate tool for analysing energy bands. Within the latter exact analytic results are obtained for the constant energy contours (CEC). These expressions are used to fit the FS of $\text{Nd}_{2-x}\text{Ce}_x\text{CuO}_{4-\delta}$ [3], $\text{Pb}_{0.42}\text{Bi}_{1.73}\text{Sr}_{1.94}\text{Ca}_{1.3}\text{Cu}_{1.92}\text{O}_{8+x}$ [6], and Sr_2RuO_4 [7] measured in angle-resolved photoemission/angle-resolved ultraviolet spectroscopy (ARPES/ARUPS) experiments.

In particular, by applying the Löwdin perturbative technique for the CuO_2 plane we give the LCAO wave function of the states near the Fermi energy ϵ_F . These states could be useful in constructing the pairing theory for CuO_2 plane. For the layered cuprates we find an alternative concerning the Fermi level location— $\text{Cu}3d_{x^2-y^2}$ *vs.* $\text{O}2p\sigma$ character of the conduction band. It is shown that analysis of extra spectroscopic data is needed in order for this dilemma to be resolved. As regards the RuO_2 plane, the existence of three pockets of the FS unambiguously reveals the $\text{Ru}4d\epsilon$ character of the conduction bands [8, 9].

To address the conduction bands in the layered perovskites we start from a common Hamiltonian including the basis of valence states $\text{O}2p$ and $\text{Ru}4d\epsilon$, or $\text{Cu}3d_{x^2-y^2}$, $\text{Cu}4s$ respectively for cuprates. Despite the equivalent crystal structure of Sr_2RuO_4 [10] and $\text{La}_{2-x}\text{Ba}_x\text{CuO}_4$ [11], the states in their conduction band(s) are, in some sense, complimentary. In other words, for the CuO_2 plane the conduction band is of σ -character while for the RuO_2 plane the conduction bands are determined by π valence bonds. This is due to the separation into σ - and π -part of the Hamiltonian $H = H^{(\sigma)} + H^{(\pi)}$ in first approximation. The latter two Hamiltonians are studied separately.

Accordingly, the paper is structured as follows. In section 2 we consider the generic $H^{(4\sigma)}$ Hamiltonian of the CuO_2 plane [12, 13] and $H^{(\pi)} = H^{(xy)} + H^{(z)}$ is then studied in section 3. The results of the comparison with the experimental data are summarised in section 4. Before embarking on a detailed analysis, however, we give an account of some clarifying issues concerning the applicability of the TB model and the band theory in general.

1.1. Apology to the band theory

It is well-known that the electron band theory is a self-consistent treatment of the electron motion in the crystal lattice. Even the classical 3-body problem demonstrates strongly correlated solutions, so it is *a priori* unknown whether the self-consistent approximation is applicable when describing the electronic structure of every new crystal. However, the one-particle band picture is an indispensable stage in the complex study of materials. It is the analysis of experimental data using a conceptually clear band theory that reveals nontrivial effects: how strong the strongly correlated electronic effects are, whether it is possible to take into account the influence of some interaction-induced order parameter back into the electronic structure etc. Therefore the comparison of the experiment with the band calculations is not an attempt, as sometimes thought, to hide the relevant issues—it is a tool to reveal interesting and nontrivial properties of the electronic structure.

Many electron band calculations have been performed for the layered perovskites and results were compared to data due to ARPES experiments. The shape of the Fermi surface is probably the simplest test to check whether we are on the right track or some conceptually new theory should be used from the very beginning.

The tight-binding interpolation of the electronic structure is often used for fitting the experimental data. This is because the accuracy of that approximation is often higher than the uncertainties in the experiment. Moreover, the tight-binding method gives simple formulae which could be of use for experimentalists to see how far they can get with such a simple minded approach. The tight-binding parameters, however, have in a sense "their own life" independent of the *ab initio* calculations. These parameters can be fitted directly to the experiment even when, by some reasons, the electron band calculations could give wrong predictions. In this sense the tight-binding parameters are the appropriate intermediary between the theory and experiment. As for the theory, establishing of reliable one-particle tight-binding parameters is the preliminary step in constructing more realistic many-body Hamiltonians. The role of the band theory is, thus, quite ambivalent: on one hand, it is the final "language" used in efforts towards understanding a broad variety of phenomena; on the other hand, it is the starting point in developing realistic interaction Hamiltonians for sophisticated phenomena such as magnetism and superconductivity.

The tight-binding method is the simplest one employed in the electron band calculations and it is described in every textbook in solid state physics; the layered

perovskites are now probably the best investigated materials and the Fermi surface is a fundamental notion in the physics of metals. There is a consensus that the superconductivity of layered perovskites is related to electron processes in the CuO_2 and RuO_2 planes of these materials. It is not, however, fair to criticise a given study, employing the tight-binding method as an interpolation scheme to the first principles calculations, for not thoroughly discussing the many-body effects. The criticism should rather be readdressed to the *ab initio* band calculations. An interpolation scheme cannot contain more information than the underlying theory. It is not erroneous if such a scheme works with an accuracy high enough to adequately describe both the theory and experiment.

In view of the above, we find it very strange that there are no simple interpolation formulae for the Fermi surfaces available in the literature and the experimental data are being published without an attempt towards simple interpretation. One of the aims of the present paper is to help interpret the experimental data by the tight-binding method as well as setting up notions in the analysis of the *ab initio* calculations.

2. Layered cuprates

2.1. Model

The CuO_2 plane appears as a common structural detail for all layered cuprates. Therefore, in order to retain the generality of the considerations, the electronic properties of the bare CuO_2 plane will be addressed without taking into account structural details such as dimpling, orthorhombic distortion, double planes, surrounding chains etc. For the square unit cell with lattice constant a_0 three-atomic basis is assumed $\{\mathbf{R}_{\text{Cu}}, \mathbf{R}_{\text{O}_b}, \mathbf{R}_{\text{O}_a}\} = \{\mathbf{0}, (a_0/2, 0), (0, a_0/2)\}$. The unit cell is indexed by vector $\mathbf{n} = (n_x, n_y)$, where $n_x, n_y = \text{integer}$. Within such an idealized model the LCAO wave function spanned over the $|\text{Cu}3d_{x^2-y^2}\rangle, |\text{Cu}4s\rangle, |\text{O}_a2p_x\rangle, |\text{O}_b2p_y\rangle$ states reads as

$$\begin{aligned} \psi_{\text{LCAO}}(\mathbf{r}) = \sum_{\mathbf{n}} \left[X_{\mathbf{n}} \psi_{\text{O}_a2p_x}(\mathbf{r} - \mathbf{R}_{\text{O}_a} - a_0 \mathbf{n}) + Y_{\mathbf{n}} \psi_{\text{O}_b2p_y}(\mathbf{r} - \mathbf{R}_{\text{O}_b} - a_0 \mathbf{n}) \right. \\ \left. + S_{\mathbf{n}} \psi_{\text{Cu}4s}(\mathbf{r} - \mathbf{R}_{\text{Cu}} - a_0 \mathbf{n}) + D_{\mathbf{n}} \psi_{\text{Cu}3d}(\mathbf{r} - \mathbf{R}_{\text{Cu}} - a_0 \mathbf{n}) \right], \end{aligned} \quad (2.1)$$

where $\Psi_{\mathbf{n}} = (D_{\mathbf{n}}, S_{\mathbf{n}}, X_{\mathbf{n}}, Y_{\mathbf{n}})$ is the tight-binding wave function in lattice representation.

The neglect of the differential overlap leads to an LCAO Hamiltonian of the CuO_2 plane

$$\begin{aligned} H = \sum_{\mathbf{n}} \left\{ D_{\mathbf{n}}^\dagger [-t_{pd}(-X_{\mathbf{n}} + X_{x-1,y} + Y_{\mathbf{n}} - Y_{x,y-1}) + \epsilon_d D_{\mathbf{n}}] \right. \\ + S_{\mathbf{n}}^\dagger [-t_{sp}(-X_{\mathbf{n}} + X_{x-1,y} - Y_{\mathbf{n}} + Y_{x,y-1}) + \epsilon_s S_{\mathbf{n}}] \\ + X_{\mathbf{n}}^\dagger [-t_{pp}(Y_{\mathbf{n}} - Y_{x+1,y} - Y_{x,y-1} + Y_{x+1,y-1}) \\ - t_{sp}(-S_{\mathbf{n}} + S_{x+1,y}) - t_{pd}(-D_{\mathbf{n}} + D_{x+1,y}) + \epsilon_p X_{\mathbf{n}}] \\ + Y_{\mathbf{n}}^\dagger [-t_{pp}(X_{\mathbf{n}} - X_{x-1,y} - X_{x,y+1} + X_{x-1,y+1}) \\ \left. - t_{sp}(-S_{\mathbf{n}} + S_{x,y+1}) - t_{pd}(D_{\mathbf{n}} + D_{x,y+1}) + \epsilon_p Y_{\mathbf{n}} \right\}, \end{aligned} \quad (2.2)$$

where the components of $\Psi_{\mathbf{n}}$ should be considered as being Fermi operators. The notations ϵ_d , ϵ_s , and ϵ_p stand respectively for the $\text{Cu}3d_{x^2-y^2}$, $\text{Cu}4s$ and $\text{O}2p\sigma$ single-site energies. The direct $\text{O}_a2p_x \rightarrow \text{O}_b2p_y$ exchange is denoted by t_{pp} and similarly t_{sp} and t_{pd} denote the $\text{Cu}4s \rightarrow \text{O}2p$ and $\text{O}2p \rightarrow \text{Cu}3d_{x^2-y^2}$ hoppings respectively. The sign rules for the hopping amplitudes are sketched in figure 1—the bonding orbitals enter the Hamiltonian with a negative sign. The latter follows directly from the surface integral approximation for the transfer amplitudes, given in Appendix A.

For the Bloch states diagonalizing the Hamiltonian (2.2)

$$\Psi_{\mathbf{n}} \equiv \begin{pmatrix} D_{\mathbf{n}} \\ S_{\mathbf{n}} \\ X_{\mathbf{n}} \\ Y_{\mathbf{n}} \end{pmatrix} = \frac{1}{\sqrt{N}} \sum_{\mathbf{p}} \begin{pmatrix} D_{\mathbf{p}} \\ S_{\mathbf{p}} \\ e^{i\varphi_a} X_{\mathbf{p}} \\ e^{i\varphi_b} Y_{\mathbf{p}} \end{pmatrix} e^{i\mathbf{p}\cdot\mathbf{n}}, \quad (2.3)$$

where N is the number of the unit cells, we use the same phases as in references [12, 13]: $\varphi_a = \frac{1}{2}(p_x - \pi)$, $\varphi_b = \frac{1}{2}(p_y - \pi)$. This equation describes the Fourier transformation between the coordinate representation $\Psi_{\mathbf{n}} = (D_{\mathbf{n}}, S_{\mathbf{n}}, X_{\mathbf{n}}, Y_{\mathbf{n}})$, with \mathbf{n} being the cell index, and the momentum representation $\psi_p = (D_p, S_p, X_p, Y_p)$ of the TB wave function (when used as an index, the electron quasi-momentum vector is denoted by p). Hence, the Schrödinger equation $i\hbar d_t \hat{\psi}_{p,\alpha} = [\hat{\psi}_{p,\alpha}, \hat{H}]$ for $\psi_{p,\alpha}(t) = e^{-ict/\hbar} \psi_{p,\alpha}$, with α being the spin index (\uparrow, \downarrow) (suppressed hereafter), takes the form

$$\left(H_p^{(4\sigma)} - \epsilon \mathbb{1} \right) \psi_p = \begin{pmatrix} -\epsilon_d & 0 & t_{pd}s_x & -t_{pd}s_y \\ 0 & -\epsilon_s & t_{sp}s_x & t_{sp}s_y \\ t_{pd}s_x & t_{sp}s_x & -\epsilon_p & -t_{pp}s_x s_y \\ -t_{pd}s_y & t_{sp}s_y & -t_{pp}s_x s_y & -\epsilon_p \end{pmatrix} \begin{pmatrix} D_p \\ S_p \\ X_p \\ Y_p \end{pmatrix} = 0, \quad (2.4)$$

where

$$\epsilon_d = \epsilon - \epsilon_d, \quad \epsilon_s = \epsilon - \epsilon_s, \quad \epsilon_p = \epsilon - \epsilon_p,$$

and

$$s_x = 2 \sin(\frac{1}{2}p_x), \quad s_y = 2 \sin(\frac{1}{2}p_y), \quad x = \sin^2(\frac{1}{2}p_x), \quad y = \sin^2(\frac{1}{2}p_y) \\ 0 \leq p_x, p_y \leq 2\pi.$$

This 4σ -band Hamiltonian is generic for the layered cuprates, cf. reference [13]. We have also included the direct oxygen-oxygen exchange t_{pp} dominated by the σ amplitude. The secular equation

$$\det \left(H_p^{(4\sigma)} - \epsilon \mathbb{1} \right) = \mathcal{A}xy + \mathcal{B}(x + y) + \mathcal{C} = 0 \quad (2.5)$$

gives the spectrum and the canonical form of the CEC with energy-dependent coefficients

$$\mathcal{A}(\epsilon) = 16(4t_{pd}^2 t_{sp}^2 + 2t_{sp}^2 t_{pp} \epsilon_d - 2t_{pd}^2 t_{pp} \epsilon_s - t_{pp}^2 \epsilon_d \epsilon_s) \\ \mathcal{B}(\epsilon) = -4\epsilon_p(t_{sp}^2 \epsilon_d + t_{pd}^2 \epsilon_s) \\ \mathcal{C}(\epsilon) = \epsilon_d \epsilon_s \epsilon_p^2. \quad (2.6)$$

Hence, the explicit CEC equation reads as

$$p_y = \pm \arcsin \sqrt{y}, \quad \text{if } 0 \leq y = -\frac{\mathcal{B}x + \mathcal{C}}{\mathcal{A}x + \mathcal{B}} \leq 1. \quad (2.7)$$

This equation reproduces the rounded square-shaped FS, centered at the (π, π) point, inherent for all layered cuprates. The best fit is achieved when \mathcal{A} , \mathcal{B} and \mathcal{C} are considered as fitting parameters. Thus, for a CEC passing through the $\mathbf{D} = (p_d, p_d)$ and $\mathbf{C} = (p_c, \pi)$ reference points, as indicated in figure 2, the fitting coefficients (distinguished by the subscript f) in the canonical equation $\mathcal{A}_f xy + \mathcal{B}_f(x + y) + \mathcal{C}_f = 0$ have the form

$$\begin{aligned}\mathcal{A}_f &= 2x_d - x_c - 1, & x_d &= \sin^2(p_d/2) \\ \mathcal{B}_f &= x_c - x_d^2, & x_c &= \sin^2(p_c/2) \\ \mathcal{C}_f &= x_d^2(x_c + 1) - 2x_c x_d,\end{aligned}\tag{2.8}$$

and the resulting LCAO Fermi contour is quite compatible with the LDA calculations for $\text{Nd}_{2-x}\text{Ce}_x\text{CuO}_{4-\delta}$ [15, 4]. Due to the simple shape of the FS the curves just coincide. We note also that the canonical equation (2.5) would formally correspond to 1-band TB Hamiltonian of a 2D square lattice of the form

$$\epsilon(\mathbf{p}) = -2t(\cos p_x + \cos p_y) + 4t' \cos p_x \cos p_y,$$

with strong energy dependence of the hopping parameters, where t' is the anti-bonding hopping between the sites along the diagonal, cf. references [16, 17].

2.2. Effective Hamiltonians

Studies of the electronic structure of the layered cuprates have unambiguously proved the existence of a large hole pocket—a rounded square centred at the (π, π) point. This observation is indicative for a Fermi level located in a single band of dominant $\text{Cu}3d_{x^2-y^2}$ character. To address this band and the related wave functions it is therefore convenient an effective Cu-Hamiltonian to be derived by Löwdin downfolding of the oxygen orbitals. This is equivalent to expressing the oxygen amplitudes from the third and fourth rows of (2.4)

$$X = \frac{1}{\eta_p} \left[t_{pd} s_X \left(1 + \frac{t_{pp}}{\varepsilon_p} s_Y^2 \right) D + t_{sp} s_X \left(1 - \frac{t_{pp}}{\varepsilon_p} s_Y^2 \right) S \right]\tag{2.9}$$

$$Y = \frac{1}{\eta_p} \left[-t_{pd} s_Y \left(1 + \frac{t_{pp}}{\varepsilon_p} s_X^2 \right) D + t_{sp} s_Y \left(1 - \frac{t_{pp}}{\varepsilon_p} s_X^2 \right) S \right],$$

where $\eta_p = \varepsilon_p - \frac{t_{pp}^2}{\varepsilon_p} s_X^2 s_Y^2$, and substituting back into the first and the second rows of the same equation. Such a downfolding procedure results in the following energy-dependent copper Hamiltonian

$$H_{\text{Cu}}(\epsilon) = \begin{pmatrix} \epsilon_d + \frac{(2t_{pd})^2}{\eta_p} (x + y + \frac{8t_{pp}}{\varepsilon_p} xy) & \frac{(2t_{pd})(2t_{sp})}{\eta_p} (x - y) \\ \frac{(2t_{pd})(2t_{sp})}{\eta_p} (x - y) & \epsilon_s + \frac{(2t_{pd})^2}{\eta_p} (x + y - \frac{8t_{pp}}{\varepsilon_p} xy) \end{pmatrix},\tag{2.10}$$

which enters the effective Schrödinger equation $H_{\text{Cu}} \begin{pmatrix} D \\ S \end{pmatrix} = \epsilon \begin{pmatrix} D \\ S \end{pmatrix}$. Thus, from (2.9) and (2.10) one can easily obtain an approximate expression for the eigenvector corresponding

to a dominant $\text{Cu}3d_{x^2-y^2}$ character. Taking $D \approx 1$, in the lowest order with respect to the hopping amplitudes t_{ij} one has

$$|\text{Cu}3d_{x^2-y^2}\rangle = \begin{pmatrix} D \\ S \\ X \\ Y \end{pmatrix} \approx \begin{pmatrix} 1 \\ (t_{sp}t_{pd}/\varepsilon_s\varepsilon_p)(s_x^2 - s_y^2) \\ (t_{pd}/\eta_p)s_x \\ -(t_{pd}/\eta_p)s_y \end{pmatrix}, \quad (2.11)$$

i.e. $|X|^2 + |Y|^2 + |S|^2 \ll |D|^2 \approx 1$. We note that within this Cu scenario the Fermi level location and the CEC shape are not sensitive to the t_{pp} parameter. Therefore one can neglect the oxygen-oxygen hopping as was done, for example, by Andersen *et al* [12, 13] (the importance of the t_{pp} parameter has been considered by Markiewicz [14]) and the band structure of the Hamiltonian (2.10) for the same set of energy parameters as used in reference [13] is shown in figure 3 (a). In this case the FS can be fitted by its diagonal alone, i.e. using only D as a reference point. Hence an equation for the Fermi energy follows, $\mathcal{A}(\epsilon_F)x_d^2 + 2\mathcal{B}(\epsilon_F)x_d + \mathcal{C}(\epsilon_F) = 0$, which yields $\epsilon_F = 2.5$ eV. As seen in figure 3 (b), the deviation from the two-parametr fit, discussed in section 2.1 is almost vanishing thus justifying the neglect of t_{pp} and using one-parametr fit.

However, despite the excellent agreement between the LDA calculations, the LCAO fit and the ARPES data regarding the FS shape, the theoretically calculated conduction band width w_c in the layered cuprates is overestimated by a factor of 2 or even 3 [3]. Such a discrepancy may well point to some alternative interpretations of the available experimental data. In the following section we shall consider the possibility for a Fermi level lying in an oxygen band.

2.2.1. Oxygen scenario: the Abrikosov-Falkovsky model Various hints currently exist in favor of O2p character of the states near the Fermi level [18, 19]. We consider that these arguments cannot be *a priori* ignored. This is best seen if, following Abrikosov and Falkovsky [20], the experimental data are interpreted within an alternative oxygen scenario.

Accordingly, the oxygen 2p level is assumed to lie above the $\text{Cu}3d_{x^2-y^2}$ level, and the Fermi level to fall into the upper oxygen band, $\epsilon_d < \epsilon_p < \epsilon_F < \epsilon_s$. The $\text{Cu}3d_{x^2-y^2}$ band is completely filled in the metallic phase and the holes are found to be in the approximately half-filled O2p σ bands. To inspect such a possibility in detail we use again the Löwdin downfolding procedure now applied to Cu orbitals. From the first and second rows of (2.4) we express the copper amplitudes

$$D = \frac{t_{pd}}{\varepsilon_d}(s_x X - s_y Y) \quad (2.12)$$

$$S = \frac{t_{sp}}{\varepsilon_s}(s_x X + s_y Y)$$

and substitute them in the third and the fourth rows. This leads to an effective oxygen Hamiltonian of the form

$$H_O(\epsilon) = B \begin{pmatrix} s_x s_x & s_x s_y \\ s_y s_x & s_y s_y \end{pmatrix} - t_{\text{eff}} \begin{pmatrix} 0 & s_x s_y \\ s_y s_x & 0 \end{pmatrix} \quad (2.13)$$

with spectrum

$$\epsilon(\mathbf{p}) = 2B(\epsilon)(x+y) \left[-1 \pm \sqrt{1 + (2\tau + \tau^2) \frac{4xy}{(x+y)^2}} \right], \quad (2.14)$$

where

$$B(\epsilon) = -\frac{t_{pd}^2}{\epsilon_d} + \frac{t_{sp}^2}{(-\epsilon_s)}, \quad t_{\text{eff}}(\epsilon) = t_{pp} + 2\frac{t_{pd}^2}{\epsilon_d}, \quad \tau(\epsilon) = t_{\text{eff}}/B \quad (2.15)$$

$$-\epsilon_s, \epsilon_d > 0 \quad (2.16)$$

and the conduction band dispersion rate $\epsilon_c(\mathbf{p})$ corresponds to the "+" sign for $|\tau| < 1$. It should be noted that (2.14) is an exact result within the adopted 4σ -band model. As a consequence, it is easily realised that along the $(0,0)$ - $(\pi,0)$ direction the conduction band is dispersionless, $\epsilon_c(p_x, 0) = 0$. This corresponds to the extended Van Hove singularity observed in the ARPES experiment [21] and we consider it being a hint in favour of the oxygen scenario (the copper model would give instead the usual Van Hove scenario).

Depending on the τ value two different limit cases occur. For $\tau \ll 1$ one gets a simple Padè approximant

$$\epsilon_c(\mathbf{p}) = 4t_{\text{eff}}(\epsilon_c) \frac{2xy}{x+y} \quad (2.17)$$

and eigenvector of $H^{(4\sigma)}$

$$|c\rangle = \begin{pmatrix} D \\ S \\ X \\ Y \end{pmatrix} \approx \frac{1}{\sqrt{s_x^2 + s_y^2}} \begin{pmatrix} \frac{2t_{pd}}{\epsilon_d} s_x s_y \\ 0 \\ -s_y \\ s_x \end{pmatrix}, \quad (2.18)$$

normalized according to the inequality $|D|^2 + |S|^2 \ll |X|^2 + |Y|^2 \approx 1$. This limit case acceptably describes the experimental ARPES data e.g. for $\text{Nd}_{2-x}\text{Ce}_x\text{CuO}_{4-\delta}$, material with single CuO_2 planes and no other complicating structural details. Schematic representation of the energy surface defined by (2.17) is shown in figure 4 (a). In figure 4 (b) we have presented a comparison between the ARPES data from reference [3] and the Fermi contour calculated according to (2.17) for $x = 0.15$. Note that *no fitting parameters* are used and this contour should be referred to as an *ab initio* calculation of the FS.

The opposite limit case $t_{\text{eff}} \gg B$, i.e. $\tau \gg 1$, has been analysed in detail by Abrikosov and Falkovsky [20]. The conduction band dispersion rate ϵ_c and the corresponding eigenvector of the Hamiltonian H_O (2.13) now take the form

$$\epsilon_c(\mathbf{p}) = 4t_{\text{eff}}(\epsilon_c)\sqrt{xy} \quad (2.19)$$

$$|c\rangle \approx \frac{1}{\sqrt{2}} \begin{pmatrix} (t_{pd}/\epsilon_d)(s_x + s_y) \\ (t_{sp}/\epsilon_s)(s_x - s_y) \\ 1 \\ -1 \end{pmatrix}, \quad (2.20)$$

provided that $|D|^2 + |S|^2 \ll |X|^2 + |Y|^2 \approx 1$. In other words, the last approximation, $\tau \gg 1$, corresponds to a pure oxygen model where only hoppings between oxygen ions

are taken into account. Clearly, this model is the complementary to the copper scenario and is based on an effect completely neglected in its copper "counterpart", where $t_{pp} \equiv 0$. This limit case of the oxygen scenario suitably describes the ARUPS experimental data for $\text{Pb}_{0.42}\text{Bi}_{1.73}\text{Sr}_{1.94}\text{Ca}_{1.3}\text{Cu}_{1.92}\text{O}_{8+x}$ [6]. The FS of the latter is fitted by its diagonal (the D point) according to the Abrikosov-Falkovsky relation (2.19) and the result is shown in figure 5.

There exist a tremendous number of ARPES/ARUPS data for layered cuprates which makes the reviewing of all those spectra impossible. To illustrate our TB model we have chosen data for the Pb substitution for Bi in $\text{Bi}_2\text{Sr}_2\text{CaCu}_2\text{O}_8$, see figure 5. In this case the CuO_2 planes are quite flat and the ARPES data are not distorted by structural details. When present, distortions were misinterpreted as a manifestation of strong antiferromagnetic correlations. We believe, however, that the experiment by Aebi *et al* [6] reveals the main feature of the CuO_2 plane band structure—the large hole pocket found to be in agreement with the one-particle band calculations.

Besides the good agreement between the theory and the experiment, regarding the FS shape, we should also point out the compatibility between the calculated and the experimental conduction bandwidth. Indeed, within the Abrikosov-Falkovsky model [20], according to (2.19), one gets for the conduction bandwidth $0 \leq \epsilon_c(\mathbf{p}) \leq w_c \approx 4t_{pp}$, which coincides with the value obtained from (2.17) provided that $t_{pd}^2 \ll t_{pp}(\epsilon_F - \epsilon_d)$. The *ab initio* calculation of t_{pp} as a surface integral (see Appendix A), making use of atomic wave functions standard for the quantum mechanical calculations, gives $t_{pp} \approx 200\text{--}350$ meV in different estimations. This range is in acceptable agreement with the experimental $w_c \simeq 1$ eV [3]; within the LCAO model an exact analytic result for w_c can be obtained from the equation $w_c = 4t_{pp} + 8t_{pd}^2/(w_c - \epsilon_d)$.

We note also that the TB analysis allows the bands to be unambiguously classified with respect to the atomic levels from which they arise. Within such terms, for the oxygen scenario one can describe the metal→insulator transition as being the charge transfer $\text{Cu}^{1+}\text{O}_2^{1\frac{1}{2}-} \rightarrow \text{Cu}^{2+}\text{O}_2^{2-}$. The possibility for monovalent copper Cu^{1+} in the superconducting state is discussed, for example, by Romberg *et al* [22].

3. Conduction bands of RuO_2 plane

Sr_2RuO_4 is the first copper-free perovskite superconductor isostructural to the high- T_c cuprates [10]. The layered ruthenates, just like the layered cuprates, are strongly anisotropic and in a first approximation the nature of the conduction band(s) can be understood by analysing the bare RuO_2 plane. One should repeat the same steps as in the previous section but now having Ru instead of Cu and the Fermi level located in the metallic bands of $\text{Ru}4d\pi$ character. To be specific, the conduction bands arise from the hybridisation between the $\text{Ru}4d_{xy}$, $\text{Ru}4d_{yz}$, $\text{Ru}4d_{zx}$ and O_a2p_y , O_b2p_x , $\text{O}_{a,b}2p_z$ π -orbitals. The LCAO wave function spanned over the four perpendicular to the RuO_2

plane orbitals reads as

$$\Psi_{\text{LCAO}}^{(z)}(\mathbf{r}) = \frac{1}{\sqrt{N}} \sum_{\mathbf{p}} \sum_{\mathbf{n}} \left[D_{zx,\mathbf{n}} \psi_{\text{Ru}4d_{zx}}(\mathbf{r} - a_0 \mathbf{n}) + D_{zy,\mathbf{n}} \psi_{\text{Ru}4d_{zy}}(\mathbf{r} - a_0 \mathbf{n}) \right. \\ \left. + e^{i\varphi_a} Z_{a,\mathbf{n}} \psi_{\text{O}_a 2p_z}(\mathbf{r} - \mathbf{R}_{\text{O}_a} - a_0 \mathbf{n}) + e^{i\varphi_b} Z_{b,\mathbf{n}} \psi_{\text{O}_b 2p_z}(\mathbf{r} - \mathbf{R}_{\text{O}_b} - a_0 \mathbf{n}) \right] e^{i\mathbf{p} \cdot \mathbf{n}}, \quad (3.1)$$

Hence, the π -analog of (2.4) takes the form

$$\left(H_p^{(z)} - \epsilon \mathbb{1} \right) \psi_p^{(z)} = \begin{pmatrix} -\varepsilon_{zx} & 0 & t_{z,zx} s_X & 0 \\ 0 & -\varepsilon_{zy} & 0 & t_{z,zy} s_Y \\ t_{z,zx} s_X & 0 & -\varepsilon_{za} & -t_{zz} c_X c_Y \\ 0 & t_{z,zy} s_Y & -t_{zz} c_X c_Y & -\varepsilon_{zb} \end{pmatrix} \begin{pmatrix} D_{zx} \\ D_{zy} \\ Z_a \\ Z_b \end{pmatrix} = 0, \quad (3.2)$$

where

$$\varepsilon_{zx} = \epsilon - \epsilon_{zx}, \quad \varepsilon_{za} = \epsilon - \epsilon_{za}, \quad c_X = 2 \cos(p_x/2), \\ \varepsilon_{zy} = \epsilon - \epsilon_{zy}, \quad \varepsilon_{zb} = \epsilon - \epsilon_{zb}, \quad c_Y = 2 \cos(p_y/2), \quad (3.3)$$

and ϵ_{zx} , ϵ_{zy} , ϵ_{za} , and ϵ_{zb} are the single site energies respectively for $\text{Ru}4d_{zx}$, $\text{Ru}4d_{zy}$ and $\text{O}_a 2p_z$, $\text{O}_b 2p_z$ orbitals. t_{zz} stands for the hopping between the latter two orbitals and, if a negligible orthorhombic distortion is assumed, the metal-oxygen π -hopping parameters are equal, $t_{z,zy} = t_{z,zx}$ and also $\epsilon_z = \epsilon_{za} = \epsilon_{zb}$. The phase factors $e^{i\varphi_{a,b}}$ in (3.1) are chosen in compliance with reference [13], see equation (2.3).

Identically, writing the LCAO wave function spanned over the three in-plane π -orbitals $\text{Ru}4d_{xy}$, $\text{O}_a 2p_y$, and $\text{O}_b 2p_x$ in the way in which (3.1) is designed one has for the "in-plane" Schrödinger equation

$$\left(H_p^{(xy)} - \epsilon \mathbb{1} \right) \psi_p^{(xy)} = \begin{pmatrix} -\varepsilon_{xy} & t_{pd\pi} s_X & t_{pd\pi} s_Y \\ t_{pd\pi} s_X & -\varepsilon_{ya} & t'_{pp} s_X s_Y \\ t_{pd\pi} s_Y & t'_{pp} s_X s_Y & -\varepsilon_{xb} \end{pmatrix} \begin{pmatrix} D_{xy} \\ Y_a \\ X_b \end{pmatrix} = 0, \quad (3.4)$$

where $t_{pd\pi}$ denotes the hopping $\text{Ru}4d_{xy} \rightarrow \text{O}_{a,b} 2p\pi$ and t'_{pp} , respectively, $\text{O}_a 2p_y \rightarrow \text{O}_b 2p_x$. The definitions for the other energy parameters are in analogy to (3.3) (for negligible orthorhombic distortion $\epsilon_{ya} = \epsilon_{xb} \neq \epsilon_z$). Thus, the π -Hamiltonian of the RuO_2 plane takes the form

$$H^{(\pi)} = \sum_{p,\alpha=\uparrow,\downarrow} \psi_{p,\alpha}^{(z)\dagger} H_p^{(z)} \psi_{p,\alpha}^{(z)} + \psi_{p,\alpha}^{(xy)\dagger} H_p^{(xy)} \psi_{p,\alpha}^{(xy)}. \quad (3.5)$$

In a previous paper [23] we have derived the corresponding secular equations and now we shall only provide the final expressions in terms of the notations used here

$$\det(H_p^{(z,xy)} - \epsilon \mathbb{1}) = \mathcal{A}^{(z,xy)} xy + \mathcal{B}^{(z,xy)}(x + y) + \mathcal{C}^{(z,xy)} = 0, \\ \mathcal{A}^{(z)} = 16(t_{z,zx}^4 - t_{zz}^2 \varepsilon_{zx}^2) \quad \mathcal{A}^{(xy)} = 32t'_{pp} t_{pd\pi}^2 - 16\varepsilon_{xy} t_{pp}^2 \\ \mathcal{B}^{(z)} = -16t_{zz}^2 \varepsilon_{zx}^2 - 4t_{z,zx}^2 \varepsilon_{zx} \varepsilon_z, \quad \mathcal{B}^{(xy)} = -t_{pd\pi}^2 \varepsilon_{ya} \\ \mathcal{C}^{(z)} = \varepsilon_{zx}^2 (\varepsilon_z^2 - 16t_{zz}^2) \quad \mathcal{C}^{(xy)} = \varepsilon_{xy} \varepsilon_{ya}^2. \quad (3.6)$$

The three sheets of the Fermi surface in Sr_2RuO_4 fitted to the ARPES data given by Lu *et al* [7] are shown in figure 6 (b). To determine the Hamiltonian parameters we have made use of the dispersion rate values at the high-symmetry points of the Brillouin

zone. To the best of our knowledge, the TB analysis of the Sr_2RuO_4 band structure was first performed in reference [23] (subsequently, the latter results were reproduced in reference [25] without referring to reference [23]). The RuO_2 -plane band structure resulting from the set of parameters

$$t_{zz} = t'_{pp} = 0.3 \text{ eV}, \quad \varepsilon_z = -2.3 \text{ eV}, \quad \varepsilon_{xy} = -1.62 \text{ eV}, \quad (3.7)$$

$$t_{pd\pi} = t_{z,zx} = 1 \text{ eV}, \quad \varepsilon_{zx} = -1.3 \text{ eV}, \quad \varepsilon_{ya,xb} = -2.62 \text{ eV}.$$

is shown in figure 6 (a). This fit is subjected to the requirement of providing as good as possible a description of the narrow energy interval around ϵ_F whereas the filled bands far below the Fermi level match only qualitatively to the LDA calculations by Oguchi [8] and Singh [9]. In addition we note that the de Haas-van Alphen (dHvA) measurements [26] of the Sr_2RuO_4 FS differ from the ARPES results [7]. Thus, fitting the dHvA data by using modified TB parameters is a natural refinement of the proposed model. We note that the diamond-shaped hole pocket, centred at the X point (see figure 6 (b)), is very sensitive to the ‘game of parameters’. For that band the van Hove energy is fairly close to the Fermi energy. As a result, a minor change in the parameters could drive a van Hove transition transforming this hole pocket to an electron one, centred at the Γ point. Indeed, such a band configuration has been recently observed also in the ARPES revision of the Sr_2RuO_4 Fermi surface [24]. This can be easily traced already from the energy surfaces $\epsilon(\mathbf{p})$ calculated earlier in reference [23]. The comparison of the ARPES data with TB energy surfaces could be a subject of a separate study.

4. Discussion

The LCAO analysis of the layered perovskites band structure, performed in the preceding sections, manifests a good compatibility with the experimental data and the band calculations as well. Due to the strong anisotropy of these materials, their FS within a reasonable approximation is determined by the properties of the bare CuO_2 or RuO_2 planes.

Despite these planes having identical crystal structure, their electronic structures are quite different. While for the RuO_2 plane the Fermi level crosses metallic π -bands, the conduction band of the CuO_2 plane is described by a σ -Hamiltonian (2.4). The latter gives for the CuO_2 plane a large hole pocket centered at the (π, π) point. Its shape, if no additional sheets exist, is well described by the exact analytic results within the LCAO model, Equation (2.5), as found for $\text{Nd}_{2-x}\text{Ce}_x\text{CuO}_{4-\delta}$ [4, 3] and $\text{Pb}_{0.42}\text{Bi}_{1.73}\text{Sr}_{1.94}\text{Ca}_{1.3}\text{Cu}_{1.92}\text{O}_{8+x}$ [6]. For a number of other cuprates, $\text{YBa}_2\text{Cu}_3\text{O}_{7-\delta}$ [27], $\text{YBa}_2\text{Cu}_4\text{O}_8$ [21], $\text{Bi}_2\text{Sr}_2\text{CaCu}_2\text{O}_8$ [28, 29], $\text{Bi}_2\text{Sr}_2\text{CuO}_6$ [30], the infinite-layered superconductor $\text{Sr}_{1-x}\text{Ca}_x\text{CuO}_2$ [31], $\text{HgBa}_2\text{Ca}_2\text{Cu}_3\text{O}_{8+\delta}$ [32], $\text{HgBa}_2\text{CuO}_{4+\delta}$ [33], $\text{HgBa}_2\text{Ca}_{n-1}\text{Cu}_n\text{O}_{2n+2+\delta}$ [34], $\text{Tl}_2\text{Ba}_2\text{Ca}_{n-1}\text{Cu}_n\text{O}_{4+2n}$, [1], $\text{Sr}_2\text{CuO}_2\text{F}_2$, $\text{Sr}_2\text{CuO}_2\text{Cl}_2$, $\text{Ca}_2\text{CuO}_2\text{Cl}_2$ [35], this large hole pocket is easily identified. For all of the above compounds, however, its shape is usually deformed due to appearance of additional sheets of the Fermi surface originating from accessoires of the crystal structure.

As the most important implication for the CuO_2 plane we should point out the intrinsic alternative about the Fermi level location (see section 2). It is commonly believed that the states at the FS are of dominant $\text{Cu}3d_{x^2-y^2}$ character (see e.g. reference [13]). Nevertheless, the spectroscopic data for the FS can be equally well interpreted within the oxygen scenario, according to which the FS states are of dominant $\text{O}2p\sigma$ character. A number of indications exist in favour of the oxygen model and the importance of the t_{pp} hopping amplitude [14, 18]:

- (i) $\text{O}1s \rightarrow \text{O}2p$ transitions observed in EELS experiments for the metallic phase of the layered cuprates, which reveal an unfilled $\text{O}2p$ atomic shell;
- (ii) the oxygen scenario reproduces in a natural way the extended van Hove singularity observed in the ARPES experiments while the Cu scenario fails to describe it;
- (iii) the metal-insulator transition can be easily described;
- (iv) the width of the conduction band is directly related to the atomic wave functions.

Some authors even "wager that the oxygen model will win" [19] (if the oxygen scenario is corroborated, due to the cancellation of the largest amplitude t_{sp} the small hoppings t_{pd} and t_{pp} should be properly evaluated eventually as surface integrals (see Appendix A) and some band calculations may well need a revision). It would be quite valuable if a muffin-tin calculation of H_2^+ ion was performed and compared with the exact results when the hopping integral is comparatively small, of the order of the one that fits the ARPES data $t_{pp} \sim 200$ meV. We also note that even the copper model gives an estimation for t_{pp} closer to the experiment than the LDA calculations. The smallness of t_{pp} within the oxygen scenario, on the other hand, is guaranteed by the nonbonding character of the conduction band. This scenario, therefore, can easily display heavy fermion behaviour, i.e. effective mass $m_{\text{eff}} \xrightarrow{t_{pp} \rightarrow 0}$ huge, and density of states (DOS) $\propto m_{\text{eff}} \propto 1/t_{pp}$ (we note that no realistic band calculations for heavy fermion systems can be performed without employing the asymptotic methods from the atomic physics). It is also instructive to compare the TB analyses of heavy fermion systems and layered cuprates. The alternative for the Fermi level location (metallic *vs.* oxygen band) exist for the cubic bismuthates as well [43, 44]. When the Fermi level falls into heavy fermion oxygen bands, one of the isoenergy surfaces is a rounded cube [43]. Indeed, such a isoenergy surface has been recently confirmed by the LMTO method applied to $\text{Ba}_{0.6}\text{K}_{0.4}\text{BiO}_3$ [45].

Due to the equally good fit of the results for the FS of the layered cuprates within the two models we can infer that at present any final judgement about this alternative would be premature. Thus far we consider that the oxygen model should be taken into account in the interpretation of the experimental data. Moreover, the angular dependence of the superconducting order parameter $\Delta(\mathbf{p}) \propto \cos(p_x) - \cos(p_y)$ is readily derived within the standard BCS treatment of the oxygen-oxygen superexchange [36]. Analysis of some extra spectroscopic data by means of different models would finally solve this dilemma. This cannot be done within the framework of the TB method. A

coherent picture requires a thorough study, where the TB model is just an useful tool to test the properties of a given solution.

Up to now, the applicability of the LCAO approximation to the electron structure of the layered cuprates can be considered as being proved. The basis function of the LCAO Hamiltonian can be included in a realistic one-electron part of the lattice Hamiltonians for the layered perovskites. This is an indispensable step preceding the inclusion of the electron-electron superexchange, electron-phonon interaction or any other kind of interaction between conducting electrons.

Acknowledgments

The authors are especially thankful to P Aebi for being so kind to provide them with extra details on ARUPS spectra as well as for the correspondence on this topic. We are much indebted to J Indekeu for the hospitality and good atmosphere during completion of this work, and would like to thank R Danev, I Genchev and R Koleva for the collaboration in the initial stages of this study. This paper was partially supported by the Bulgarian NSF No. 627/1996, the Belgian DWTC, the Flemish Government Programme VIS/97/01, the IUAP and the GOA.

Appendix A. Calculation of O-O hopping amplitude by the surface integral method

From quantum mechanics [37] it is well known that the usual for the quantum chemistry calculation of the hopping integrals as matrix elements of the single particle Hamiltonian does not work when the overlap between the atomic functions is too weak. If the hopping integrals are much smaller than the detachment energy, they should be calculated as surface integrals using (eventually distorted by the polarisation) atomic wave functions.

Such an approach has been applied by Landau and Lifshitz [37] and Herring and Flicker [38] to the simple H_2^+ problem and now the asymptotic methods are well developed in the physics of atomic collisions [39]. On the basis of the above problem one can easily verify that the atomic sphere muffin-tin approximation of the Coulomb potentials usual for the condensed matter physics undergoes *fiasco* when the hopping integrals are of the order of 200–300 meV. Therefore, the factor 2–3 misfit for a single electron problem cannot be ascribed to the strong-correlation effects, renormalizations and other incantations which are often used to account for the discrepancy between the experimental bandwidth and the LDA calculations.

Usually condensed matter physics does not need asymptotically accurate methods for calculation of hopping integrals which leads to zero overlap between the muffin-tin and asymptotic methods. However, for the perovskites the largest hopping t_{sp} cancels in the expression for the upper oxygen band $\epsilon_c(\mathbf{p})$. Thus, small hoppings become essential, but having no influence on the other bands, and the necessity of taking into account the t_{pp} is of topological nature.

Following the calculations for H_2^+ [37], in a simplified picture of two oxygen atoms O_a, O_b separated by distance $d = \frac{\sqrt{2}}{2}a_0$ the surface integral method gives for the oxygen-oxygen exchange the following explicit expression

$$t_{pp} = \frac{\hbar^2}{2m} \iint_{\mathcal{S}} (\psi_{\text{O}_a} \partial_z \psi_{\text{O}_b} - \psi_{\text{O}_b} \partial_z \psi_{\text{O}_a}) dx dy, \quad (\text{A.1})$$

where the integral is taken over the surface \mathcal{S} halving d , and m is the electron mass. Thus $t_{pp} = t_{pp}(\xi)$ is a function of $\xi = \kappa |\mathbf{R}_{\text{O}_a} - \mathbf{R}_{\text{O}_b}|$ with $\kappa^2/2$ being the oxygen detachment energy in atomic units and the detailed derivation of (A.1) can be found, for example, in reference [39].

We note that the derivation of $t_{pp}(\xi)$ imposes no restrictions on the basis set $\{\psi\}$ used. Hence we choose $\{\psi_{\text{O}_{a,b}}\}$ to be the simplest minimal (MINI) basis used [40], for example, in the GAMESS package for doing *ab initio* electronic structure calculations [41]. The MINI bases are three Gaussian expansions of each atomic orbital. The exponents and contraction coefficients are optimised for each element, and the s and p exponents are not constrained to be equal.

Accordingly, the oxygen $2p$ radial wave function $R_{2p}(r)$ is replaced by a Gaussian expansion $R_{2p}^{(G)}(r)$ and has the form

$$R_{2p}^{(G)}(\zeta, \mathbf{r}) = \sum_{i=1}^3 C_{2p,i} g_{2p,i}(\zeta_{2p,i}, \mathbf{r}), \quad (\text{A.2})$$

where $g_{2p}(\zeta, \mathbf{r}) = A_{2p,i} e^{-\zeta_{2p,i} r^2}$, and the coefficients for oxygen are given in table 1. It is then normalized to unity according to $\int_0^\infty R_{2p}^{(G)2} r^2 dr = 1$.

By multiplying with the corresponding cubic harmonic the oxygen wave functions are brought into the form

$$\psi_{\text{O}_a}(\mathbf{r}_a) = R_{2p}^{(G)}(\zeta, \mathbf{r}_a) \sqrt{\frac{3}{4\pi}} \frac{x_a}{r_a}, \quad \begin{cases} \mathbf{r}_a = \mathbf{r} - \mathbf{R}_{\text{O}_a} \\ r_a = |\mathbf{r}_a| \end{cases}, \quad (\text{A.3})$$

and analogically for $\psi_{\text{O}_b}(\mathbf{r} - \mathbf{R}_{\text{O}_b})$. Substituting (A.3) in (A.1) we get

$$t_{pp}^{(\text{MINI})} = 340 \text{ meV}.$$

In reference [42] the same integral has been calculated with $\{\psi\}$ being the asymptotic wave functions [39] appropriately tailored to the MINI basis at their outermost inflection points $r^{(i)}$, i.e.

$$R_{2p}(r) = \begin{cases} R_{2p}^{(G)}(r), & r \leq r^{(i)} \\ A \frac{\sqrt{2\kappa}}{r} e^{-\kappa r}, & r \geq r^{(i)} \end{cases} \quad (\text{A.4})$$

with $\kappa = 0.329$ and $A = 0.5$. The value obtained is

$$t_{pp}^{(\text{asympt})} = 210 \text{ meV},$$

found to be in good agreement with that fitted from the ARPES experiment within the oxygen scenario. Similar calculation, for example, gives for the t_{pd} and t_{sp} hoppings

$$t_{pd}^{(\text{MINI})} = 580 \text{ meV}, \quad t_{sp}^{(\text{MINI})} \sim 2.5 \text{ eV}.$$

Note added in proof. In a very recent paper by Campuzano J C *et al* 1999 [*Phys. Rev. Lett.* **83** 3709] the ARPES Fermi surface of pure $\text{Bi}_2\text{Sr}_2\text{CaCu}_2\text{O}_{8+\delta}$ has been presented in the inset of their figure 1 (a). This experimental finding is in excellent agreement with our tight-binding fit to the Fermi surface of $\text{Pb}_{0.42}\text{Bi}_{1.73}\text{Sr}_{1.94}\text{Ca}_{1.3}\text{Cu}_{1.92}\text{O}_{8+x}$, studied by Schwaller P and co-workers in reference 6, given in figure 5 of the present paper. The remarkable coincidence of the Fermi surfaces of these two compounds is a nice confirmation that Pb substitution for Bi is irrelevant for the band structure of the CuO_2 plane and the Fermi surface of the latter is therefore revealed to be a common feature.

References

- [1] Pickett W E, 1989 *Rev. Mod. Phys.* **61** 433
- [2] Shen Z - X and Dessau D S, 1995 *Phys. Rep.* **253** 1-162; Lynch D W and Olson C G 1999 *Photoemission studies of High-Temperature Superconductors* (Cambridge University Press)
- [3] King D M, Shen Z-X, Dessau D S, Wells B O, Spicer W E, Arko A J, Marshall D S, DiCarlo J, Loeser A G, Park C H, Ratner E R, Peng J L, Li Z Y and Greene R L, 1993 *Phys. Rev. Lett.* **70** 3159
- [4] Yu J and Freeman A J, 1991 *NASA Conf Publication 3100, Proc of a Conf on "Advances in Materials Science and Applications of High Temperature Superconductors" held at Goddard Space Flight Center, Greenbelt, Maryland, April 2-6, 1990*, ed Bennett L H *et al* (US Government Printing Office), pp 365-371
- [5] For a nice review on the tight-binding method see Goringe C M, Bowler D R and Hernández E, 1997 *Rep. Prog. Phys.* **60** 1447; Bullett D W, 1980 *Solid State Physics Series* **35** 129; Eschrig H 1989 *Optimized LCAO Method and the Electronic Structure of Extended Systems I* (Berlin: Springer)
- [6] Aebi P, Osterwalder J, Schwaller P, Schlapbach L, Shimoda M, Mochiku T and Kadowaki K, 1994 *Phys. Rev. Lett.* **72** 2757; 1995 *Phys. Rev. Lett.* **74** 1886; Osterwalder J, Aebi P, Schwaller P, Schlapbach L, Shimoda M, Mochiku T and Kadowaki K, 1995 *Appl Phys A* **60** 247; Aebi P, Osterwalder J, Schwaller P, Schlapbach L, Shimoda M, Mochiku T, Kadowaki K, Berger H and Lévy F, 1994 *Physica C* **235-240** 949; Schwaller P, Aebi P, Berger H, Beeli C, Osterwalder J and Schlapbach L 1995 *Journal of Electron Spectroscopy and Related Phenomena* **76** 127
- [7] Lu D H, Schmidt M, Cummins T R, Schuppler S, Lichtenberg F, and Bednorz J G, 1996 *Phys. Rev. Lett.* **76** 4845
- [8] Oguchi T, 1995 *Phys. Rev. B* **51** 1385
- [9] Singh D J, 1995 *Phys. Rev. B* **52** 1358
- [10] Maeno Y, Hashimoto H, Yoshida K, Nashizaki S, Fujita T, Bednorz J G, and Lichtenberg F, 1994 *Nature (London)* **372** 532
- [11] Bednorz J G and Müller K A, 1986 *Z. Phys. B* **64** 189
- [12] Andersen O K, Jepsen O, Liechtenstein A I and Mazin I I, 1994 *Phys. Rev. B* **49** 4145; Andersen O K, Savrazov S Y, Jepsen O, and Liechtenstein A I, 1996 *J. Low Temp. Phys.* **105** 285 and references therein
- [13] Andersen O K, Liechtenstein A I, Jepsen O and Paulsen F, 1995 *J. Phys. Chem. Solids* **56** 1573
- [14] Markiewicz R S, 1997 *J. Phys. Chem. Solids* **58** 1179, Sec. 5
- [15] Massidda S, Hamada N, Yu J and Freeman A J, 1989 *Physica C* **157** 571
- [16] Yu J, Freeman A J, 1991 *J. Phys. Chem. Solids* **52** 1351
- [17] Radtke R J, Levin K, Schüttler H-B, and Norman M R, 1993 *Phys. Rev. B* **48** 15957; Radtke R J and Norman M R, 1994 *Phys. Rev. B* **50** 9554
- [18] Stechel E B and Jennison D R, 1988 *Phys. Rev. B* **38** 4632; 1988 *ibid* **38** 8873; Takahashi T, Matsuyama H, Katayama-Yoshida H, Okabe Y, Hosoya S, Seki K, Fujimoto H, Sato M and

- Inokuchi H, 1988 *Nature* **334** 691; Tanaka M, Takahashi T, Katayama-Yoshida H, Yamazaki S, Fujinami M, Okabe Y, Mizutani W, Ono M and Kajimura K, 1989 *Nature* **339** 691 Takahashi T, in Springer Series in Solid State Sciences **89**, 1989 *Strong Correlation and Superconductivity*, Editors: Fukuyama A *et al* (Berlin, Heidelberg: Springer-Verlag), p 311
- [19] Blackstead H A and Dow J D, 1997 *Physica C* **282–287** 1513
- [20] Abrikosov A A and Falkovsky L A, 1990 *Physica C* **168** 556
- [21] Gofron K, Campuzano J C, Abrikosov A A, Lindroos M, Bansil A, Ding H, Koelling D and Dobrovski B, 1994 *Phys. Rev. Lett.* **73** 3302
- [22] Romberg H, Nücker N, Alexander M, Fink J, Hahn D, Zetterer T, Otto H H and Renk K F, 1990 *Phys. Rev. B* **41** 2609; Nücker N, Romberg H, Alexander M and Fink J 1990 *Electronic Structure Studies of High- T_c Cuprate Superconductors by Electron Energy-Loss Spectroscopy in Studies of High Temperature superconductors vol 6* ed A Narlikar (New York: Nova Science Publishers)
- [23] Mishonov T M, Genchev I N, Koleva R K and Penev E, 1996 *J. Low Temp. Phys.* **105** 1611; 1996 *Czech. J. Phys.* **46** 953, Suppl. S2
- [24] Puchkov A V, Shen Z-X, Kimura T and Tokura Y, 1998 *Phys. Rev. B* **58** R13322
- [25] Noce C and Cuoco M, 1999 *Phys. Rev. B* **59** 2659
- [26] Makenzie A P, Julian S R, Diver A J, McMullan G J, Ray M P, Lonzarich G G, Maeno Y, Nishizaki S and Fujita T, 1996 *Phys. Rev. Lett.* **76** 3786
- [27] Yu J, Massidda S, Freeman A J and Koeling D D, 1987 *Phys Lett A* **122** 203
- [28] Marshall D S, Dessau D S, King D M, Park C-H, Matsuura A Y, Shen Z-X, Spicer W E, Eckstein J N and Bozovic I, 1995 *Phys. Rev. B* **52** 12548; Ding H, Bellman A F, Campuzano J S, Randeria M, Norman M R, Yokoya T, Takahashi T, Katayama-Yoshida H, Mochiku T, Kadowaki K, Jennings J and Brivio G P, 1996 *Phys. Rev. Lett.* **76** 1533
- [29] Massidda S, Yu Jaejun and Freeman A J, 1988 *Physica C* **158** 251
- [30] Singh D J and Pickett W E, 1995 *Phys. Rev. B* **51** 3128
- [31] Novikov D L, Gubanov V A and Freeman A J, 1993 *Physica C* **210** 301
- [32] Singh D J and Pickett W E, 1994 *Physica C* **233** 237; 1994 *Phys. Rev. Lett.* **73** 476
- [33] Novikov D L and Freeman A J, 1993 *Physica C* **212** 233
- [34] Novikov D L and Freeman A J, 1993 *Physica C* **216** 273
- [35] Novikov D L, Freeman A J and Jorgensen J D, 1995 *Phys. Rev. B* **51** 6675
- [36] Mishonov T M and Donkov A A, 1996 *Czech. J. Phys.* **46** Suppl. 2 1051; Mishonov T M, Donkov A A, Koleva R K and Penev E 1997 *Bulgarian J. Phys.* **24** 114; Mishonov T M and Donkov A A 1997 *J. Low Temp. Phys.* **107** 541
- [37] Landau L D and Lifshitz E M, 1974 *Theoretical Physics Vol 3: Quantum Mechanics* (in russian) (Moscow: Nauka)
- [38] Herring C and Flicker M, 1964 *Phys. Rev.* **134A** 362
- [39] Smirnov B M, 1973 *Asymptotic methods in the theory of atomic collisions*, in russian (Moscow: Energoatomizdat)
- [40] Huzinaga S, Andzelm J, Klobukowski M, Radzio-Andzelm E, Sakai Y, and Tatewaki H, 1984 *Gaussian Basis Sets for Molecular Calculations* (Amsterdam: Elsevier)
- [41] Schmidt M W, Baldrige K K, Boatz J A, Jensen J H, Koseki S, Gordon M S, Nguyen K A, Windus T L, Elbert S T, 1992 *QCPE Bulletin* **10** 52
- [42] Mishonov T M, Koleva R K, Genchev I N, and Penev E, 1996 *Czech. J. Phys.* **46** 2645, Suppl. S5
- [43] Mishonov T, Genchev I, Koleva R, and Penev E, 1997 *Superlattices and Microstructures* **21** 471
- [44] Mishonov T, Genchev I, and Penev E, 1997 *Superlattices and Microstructures* **21** 477
- [45] Meregalli V and Savrazov Y, 1998 *Phys. Rev. B* **57** 14453

Figure captions

Figure 1. Schematic of a CuO_2 plane (only orbitals relevant to the discussion are depicted). The solid square represents the unit cell with respect to which the positions of the other cells are determined. The indices of the wave function amplitudes involved in the LCAO Hamiltonian (2.2) are given in brackets. The rules for determining the signs of hopping integrals t_{pd} , t_{sp} , and t_{pp} are shown as well.

Figure 2. LDA Fermi contour of $\text{Nd}_{2-x}\text{Ce}_x\text{CuO}_{4-\delta}$ (dotted line) calculated by Yu and Freeman [4] (with the kind permission of the authors), and the LCAO fit (solid line) according to (2.5). The fitting procedure uses C and D as reference points.

Figure 3. (a) Electron band structure of the generic for the CuO_2 plane 4σ -band Hamiltonian using the parameters from reference [13] and the Fermi level $\epsilon_F = 2.5$ eV fitted from the LDA calculation by Yu and Freeman [4]; (b) The LCAO Fermi contour (solid line) fitted to the LDA Fermi surface (dashed line) for $\text{Nd}_{2-x}\text{Ce}_x\text{CuO}_{4-\delta}$ [4] using only D as a reference point. The deviation of the fit at the C point is negligible.

Figure 4. (a) Energy dispersion of the nonbonding oxygen band $\epsilon_c(\mathbf{p})$, equation (2.17). A few cuts through the energy surface, i.e. CEC, are presented together with the dispersion along the high symmetry lines in the Brillouin zone; (b) The Fermi surface of $\text{Nd}_{2-x}\text{Ce}_x\text{CuO}_{4-\delta}$ (solid line) determined by equation (2.17) for $x = 0.15$ (shaded slice in panel (a)) and compared with experimental data (points with error bars) for the same value of x after King *et al* [3]. θ and φ denote the polar and azimuthal emission angles, respectively, measured in degrees. The empty dashed circles show \mathbf{k} -space locations where ARPES experiments have been performed (cf. figure 2 in reference [3]) and their diameter corresponds to 2° experimental resolution.

Figure 5. (a) ARUPS Fermi surface of $\text{Pb}_{0.42}\text{Bi}_{1.73}\text{Sr}_{1.94}\text{Ca}_{1.3}\text{Cu}_{1.92}\text{O}_{8+x}$ by Aebi *et al* [6]; (b) LCAO fit to (a) according to the Abrikosov-Falkovsky model [20] using the D reference point with $p_d = 0.171 \times 2\pi$.

Figure 6. (a) LCAO band structure of Sr_2RuO_4 according to (3.5). The Fermi level (dashed line) crosses the three $\text{Ru}4d\epsilon$ bands of the RuO_2 plane; (b) LCAO fit (solid lines) to the ARPES data (circles) by Lu *et al* [7], cf. also reference [23].

Tables and table captions

Table 1. Coefficients for the oxygen 2*p* wave function in the MINI basis [41].

i	$C_{2p,i}$	$A_{2p,i}$	$\zeta_{2p,i}$
1	8.2741400	2.485782	0.708520
2	1.1715463	1.333720	0.476594
3	0.3030130	0.263299	0.130440

Figure 1.

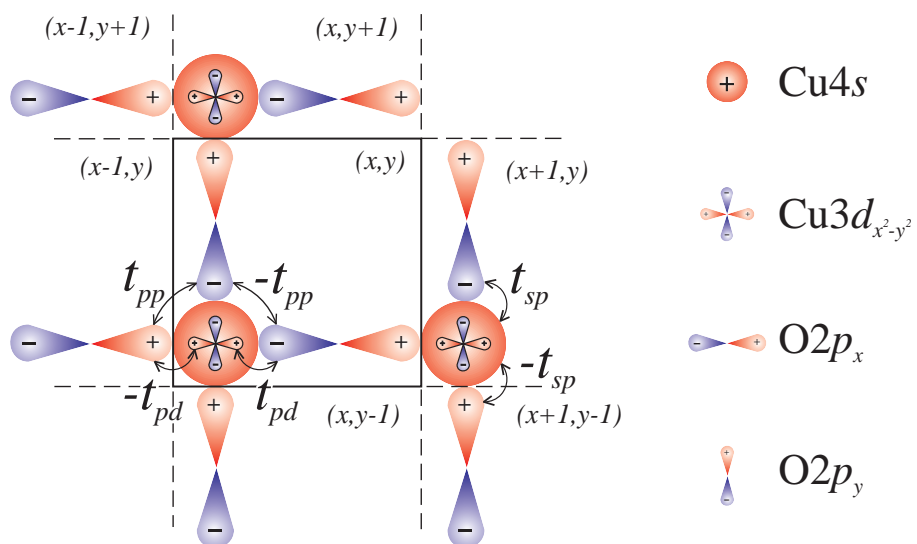


Figure 2.

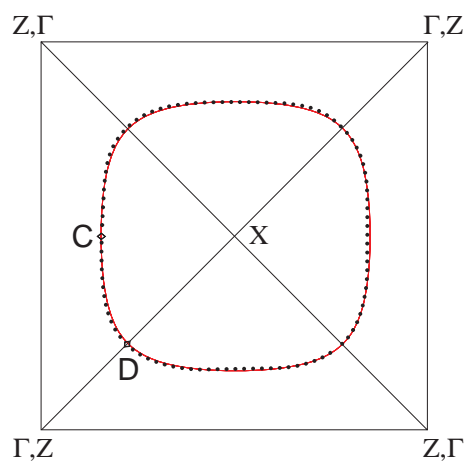


Figure 3.

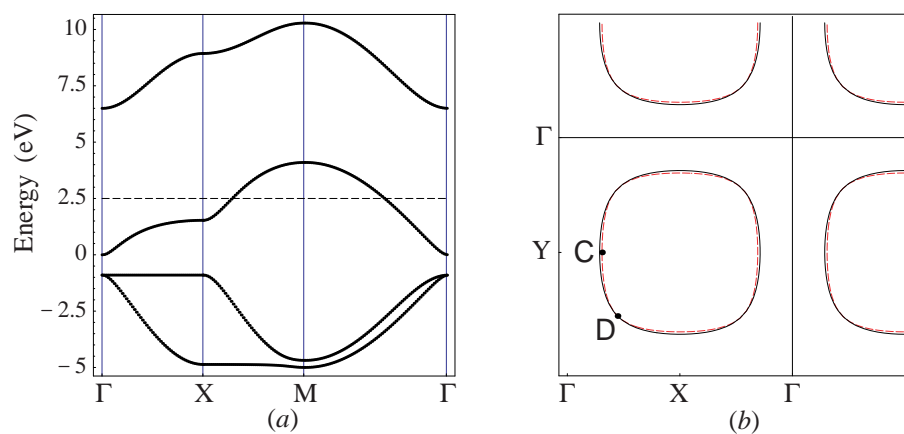


Figure 4.

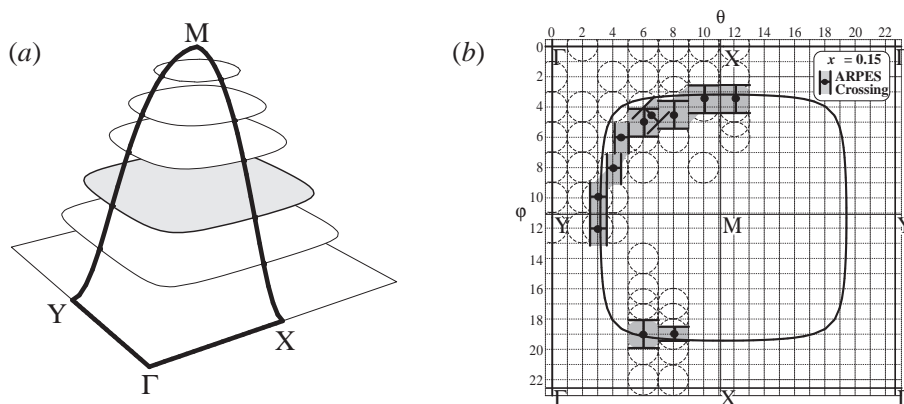


Figure 5.

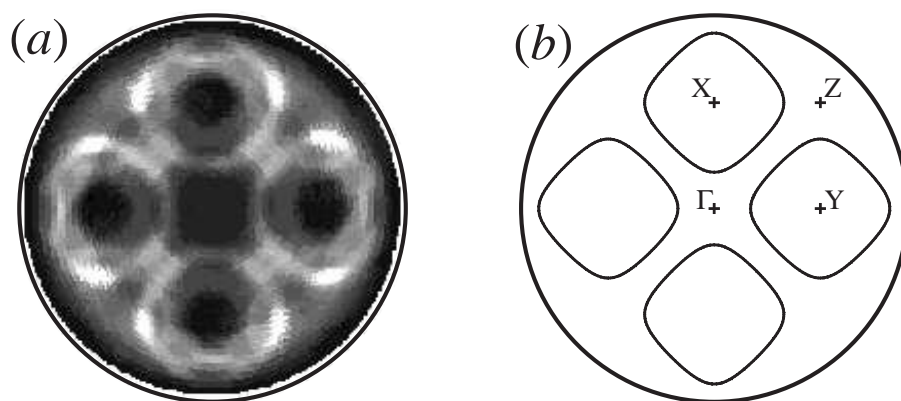


Figure 6.

